EBioMedicine 54 (2020) 102729

Contents lists available at ScienceDirect

EBioMedicine

journal homepage: www.elsevier.com/locate/ebiom

Research paper

First-in-human PeriCord cardiac bioimplant: Scalability and GMP manufacturing of an allogeneic engineered tissue graft

Cristina Prat-Vidal[a,b,c,d], Luciano Rodríguez-Gómez[e], Miriam Aylagas[e,f], Nuria Nieto-Nicolau[g], Paloma Gastelurrutia[a,b,c,d], Elba Agustí[g], Carolina Gálvez-Montón[a,b,c], Ignasi Jorba[h], Albert Teis[b], Marta Monguió-Tortajada[a,i], Santiago Roura[a,b,c], Joaquim Vives[e,j,k], Silvia Torrents-Zapata[e], María Isabel Coca[e], Laura Reales[e], María Luisa Cámara-Rosell[b], Germán Cediel[b], Ruth Coll[l], Ramon Farré[m], Daniel Navajas[h], Anna Vilarrodona[g], Joan García-López[l], Christian Muñoz-Guijosa[b], Sergi Querol[e,f], Antoni Bayes-Genis[a,b,c,k,*]

[a] ICREC Research Program, Germans Trias i Pujol Health Science Research Institute, Can Ruti Campus, Badalona, Spain
[b] Heart Institute (iCor), Germans Trias i Pujol University Hospital, Carretera de Canyet s/n, 08916 Badalona, Spain
[c] CIBER Cardiovascular, Instituto de Salud Carlos III, Madrid, Spain
[d] Institut d'Investigació Biomèdica de Bellvitge - IDIBELL, L'Hospitalet de Llobregat, Spain
[e] Cell Therapy Service, Banc de Sang i Teixits, Edifici Dr. Frederic Duran i Jordà, Passeig Taulat, 116, 08005 Barcelona, Spain
[f] Transfusional Medicine Group, Vall d'Hebron Research Institute, Autonomous University of Barcelona, Barcelona, Spain
[g] Barcelona Tissue Bank (BTB), Banc de Sang i Teixits (BST), Barcelona, Spain
[h] Institute for Bioengineering of Catalonia (IBEC), The Barcelona Institute of Science and Technology, CIBERES, University of Barcelona, Barcelona, Spain
[i] REMAR-IVECAT Group, Germans Trias i Pujol Health Science Research Institute, Can Ruti Campus, Badalona, Spain
[j] Musculoskeletal Tissue Engineering Group, Vall d'Hebron Research Institute (VHIR), Autonomous University of Barcelona, Passeig de la Vall d'Hebron 129-139, 08035 Barcelona, Spain
[k] Departament de Medicina, Universitat Autònoma de Barcelona, Passeig de la Vall d'Hebron 129-139, 08035 Barcelona, Spain
[l] Research and Education. Banc de Sang i Teixits, Edifici Dr. Frederic Duran i Jordà, Passeig Taulat, 116, 08005 Barcelona, Spain
[m] Unit of Biophysics and Bioengineering, School of Medicine and Health Sciences, University of Barcelona-IDIBAPS-CIBERES, Barcelona, Spain

ARTICLE INFO

Article History:
Received 17 December 2019
Revised 24 February 2020
Accepted 5 March 2020
Available online xxx

Keywords:
Wharton's jelly-derived mesenchymal stromal cells (WJ-MSCs)
Biofabrication
Advanced therapy medicinal product (ATMP)
Cardiac tissue engineering
Scaffold
Myocardial infarction

ABSTRACT

Background: Small cardiac tissue engineering constructs show promise for limiting post-infarct sequelae in animal models. This study sought to scale-up a 2-cm^2 preclinical construct into a human-size advanced therapy medicinal product (ATMP; PeriCord), and to test it in a first-in-human implantation.
Methods: The PeriCord is a clinical-size (12–16 cm^2) decellularised pericardial matrix colonised with human viable Wharton's jelly-derived mesenchymal stromal cells (WJ-MSCs). WJ-MSCs expanded following good manufacturing practices (GMP) met safety and quality standards regarding the number of cumulative population doublings, genomic stability, and sterility. Human decellularised pericardial scaffolds were tested for DNA content, matrix stiffness, pore size, and absence of microbiological growth.
Findings: PeriCord implantation was surgically performed on a large non-revascularisable scar in the inferior wall of a 63-year-old male patient. Coronary artery bypass grafting was concomitantly performed in the non-infarcted area. At implantation, the 16-cm^2 pericardial scaffold contained $12{\cdot}5 \times 10^6$ viable WJ-MSCs (85·4% cell viability; <0·51 endotoxin units (EU)/mL). Intraoperative PeriCord delivery was expeditious, and secured with surgical glue. The post-operative course showed non-adverse reaction to the PeriCord, without requiring host immunosuppression. The three-month clinical follow-up was uneventful, and three-month cardiac magnetic resonance imaging showed ~9% reduction in scar mass in the treated area.
Interpretation: This preliminary report describes the development of a scalable clinical-size allogeneic PeriCord cardiac bioimplant, and its first-in-human implantation.
Funding: La Marató de TV3 Foundation, Government of Catalonia, Catalan Society of Cardiology, "La Caixa" Banking Foundation, Spanish Ministry of Science, Innovation and Universities, Institute of Health Carlos III, and the European Regional Development Fund.

* Corresponding author at: Heart Institute (iCor), Germans Trias i Pujol University Hospital, Carretera de Canyet s/n, 08916 Badalona (Barcelona), Spain.
E-mail address: abayesgenis@gmail.com (A. Bayes-Genis).

https://doi.org/10.1016/j.ebiom.2020.102729

Research in context

Evidence before this study

MI sequelae remain a major cause of morbidity and mortality. Small-sized cardiac tissue engineered grafts proved safe and effective in the MI swine model.

Added value of this study

Here we developed and performed the first-in-human surgery of a scalable clinical-size PeriCord cardiac bioimplant.

Implications of all the available evidence

The PeriCord, composed of human WJ-MSCs within decellularised pericardium, was feasible and preliminarily safe, without requirement of host immunosuppression after implantation. Long-term follow up and completion of the PERISCOPE trial will confirm the value of this first-in-class PeriCord cardiac bioimplant.

1. Introduction

Myocardial infarction (MI) causes irreversible cardiac muscle loss, non-contractile scar formation, and, ultimately, a maladaptive adverse ventricular remodelling resulting in end-stage ischemic heart failure [1]. Over recent decades, many small-scale clinical trials have tested cell-based therapies using distinct cell sources, with the aim of regenerating infarcted hearts [2–5]. Many of these trials have reported only modest improvements in cardiac function, which are unlikely to be clinically relevant [6].

Main sources of mesenchymal stromal cells (MSCs) include bone marrow, adipose tissue, and Wharton's jelly from the umbilical cord discarded after birth. Notably, large quantities of allogeneic MSCs can be most easily collected from Wharton's jelly, and these Wharton's jelly-derived MSCs (WJ-MSCs) are more primitive than MSCs derived from more mature tissue sources, exhibiting intermediate properties between those of embryonic and adult stem cells [7]. Moreover, WJ-MSCs have a lower risk of carrying somatic mutations, extensive expansion capacity in culture, immunological immaturity, and immunomodulatory properties, making them optimal candidates for allogeneic cell therapy. Nevertheless, the mechanisms of action of MSCs are not fully deciphered. MSCs are associated with regenerative and immunomodulatory capabilities, including monocyte modulation toward an anti-inflammatory phenotype that facilitates tissue repair [8,9]. We observed that WJ-MSCs polarise monocytes towards a regulatory M2 phenotype, and strongly inhibit inflammatory responses of stimulated allogeneic T cells [10,11].

Cardiac tissue engineering is a therapeutic strategy that involves delivery of both cells and supportive biomaterials into injured myocardium, thus improving cell retention and survival compared with direct cell injection delivery [12,13]. We previously demonstrated that a small (2 cm^2) engineered preclinical cardiac graft comprising human decellularised pericardium and MSCs was safe and effective in an MI porcine model [14–16]. Once implanted over the ischemic myocardium, the graft became vascularised and innervated, promoting damaged tissue revascularisation, reducing infarct size, ameliorating the adverse remodelling process and fibrosis progression, and ultimately improving cardiac function [14–16].

In the present study, we describe the translational process to the clinic, including graft scalability and good manufacturing practice (GMP) biofabrication, from a small-size preclinical construct to an allogeneic investigational advanced therapy medicinal product (ATMP; named PeriCord). We also report preliminary safety data from the first PeriCord implantation performed in a roll-in patient from the ongoing phase I PERISCOPE (the PERIcardial matrix with mesenchymal Stem Cells fOr the treatment of PatiEnts with infarcted myocardial tissue) clinical trial (EudraCT N°. 2018-001964-49; ClinicalTrials.gov identifier: NCT03798353).

2. Materials and methods

2.1. Rational of the study

The main objective of this study was to scale up a small-size preclinical construct into a human-size allogeneic investigational ATMP, named PeriCord, following GMP-compliant procedures and to test it in a first-in-human implantation in the context of the PERISCOPE clinical trial (Fig. 1). This novel ATMP combines WJ-MSCs as active ingredient and human decellularised, lyophilised, and sterilised pericardium, acting as a cell supportive material (vehicle) for surgical implantation.

Umbilical cord (UC) samples were collected within the Concordia Program (http://www.bancsang.net/professionals/en_concordia) with appropriate donor informed consent. UC-mesenchymal stromal cells (MSCs) were derived from the Wharton's jelly (WJ) in qualified areas of Blood and Tissue Bank of Catalonia (BST, Barcelona), following GMP-compliant procedures. Human pericardium samples were obtained from

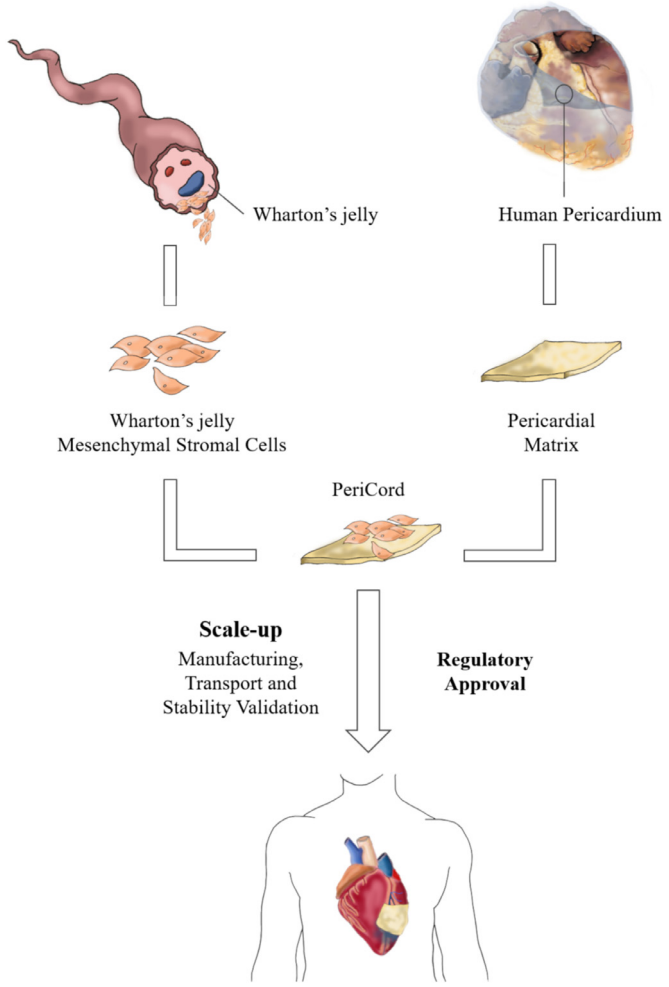

Fig. 1. Schematic of the two components of the PeriCord bioimplant, human WJ-MSCs and human decellularised pericardium. The PeriCord was safely implanted in a first-in-human patient.

deceased donors and personal information were treated in accordance with European Tissue and Cell Directives (2004/23/CE, 2006/17/CE, and 2006/86/CE), and with the local legal requirements and the Laws for the Development and Applications of Organ Transplants. Informed consent was obtained for clinical application and/or applied research.

With respect to active ingredient, we obtained $n = 4$ batches of clinical-grade WJ-MSCs. In all cases, serological, microbiological, and adventitious virus testing, karyotyping, sterility, *Mycoplasma*, endotoxin levels, phenotypic profiling and immunomodulatory assay, were performed throughout manufacturing process in order to confirm WJ-MSCs' identity and potency, to ensure batch-to-batch bioequivalence, and to guarantee suitability for clinical use. Viability of initial thawed WJ-MSCs ($n = 37$), following sucrose resuspension ($n = 37$) and after 16 h at 2–8 °C ($n = 20$) were also analysed by flow cytometry.

Concerning vehicle component, a total of $n = 35$ human pericardia were cut and decellularised. Different square pieces of ~16 cm^2 and ~1 cm^2 obtained from each pericardium were randomly assigned to different experimental sets, as follows: $n = 5$ pieces, to measure the effect of decellularisation on pericardial matrix dimensions; $n = 4$ pairs of both sizes, to quantify DNA residual content after decellularisation; $n = 4$ pieces, for histological and immunohistochemical analysis; $n = 4$ pairs of both sizes, for mechanical testing; $n = 11$ pieces, to analyse pore size and roundness ratio in decellularised pericardial matrices; and $n = 4$ pairs of both sizes, for validation of the final decellularisation protocol. Upon validation of decellularisation, $n = 3$ pericardia were used to validate manufacturing procedure of the vehicle (final matrix), including serological and microbiological testing, sterility assessment, final quadrangular size, residual moisture, and citotoxicity testing.

During the scale-up process, $n = 37$ matrix colonisations were performed using post-thawed sucrose-conditioned WJ-MSCs. After sequential cell seeding, WJ-MSCs viability was verified in samples of both ~16 cm^2 and ~1 cm^2 from $n = 3$ vehicle batches. Following the defined manufacturing protocol, WJ-MSCs' colonisation efficiency ($n = 47$), dose range ($n = 47$), and viability ($n = 27$) were determined in the finished product (FP). Finally, PeriCord's manufacturing process ($n = 4$), stability ($n = 3$) and transportation ($n = 3$) were also validated at room temperature (RT) before the first PeriCord manufactured to be implanted in a roll-in patient of the PERISCOPE trial.

2.2. Investigational medicinal product: the PeriCord

2.2.1. Active ingredient: clinical-grade WJ-MSCs

WJ-MSCs were derived from specifically donated umbilical cord tissue following previously described GMP-compliant procedures [17] in the classified areas of the Blood and Tissue Bank of Catalonia (BST; Barcelona, Spain). Briefly, clinical-grade WJ-MSCs were obtained using a two-tiered cell banking system comprising an initial master cell bank (MCB), and a second cell bank, named drug product (DP), containing ready-to-use pure WJ-MSCs. Immediately after cell expansion, DP was cryopreserved in units containing $2{\cdot}5 \times 10^7 \pm 20\%$ cells/cryovial in Plasmalyte®148 (Baxter, Deerfield, IL, USA) supplemented with 4% w/v human serum albumin (Grifols, Barcelona, Spain) and 10% v/v dimethyl sulfoxide (Cryoserv®, Bioniche Pharma, Lake Forest, IL, USA), and stored until PeriCord manufacturing.

All DP batches were assayed for identity (phenotype) and potency (immunomodulatory potential) to ensure bioequivalence between batches. Phenotype was evaluated by flow cytometry. WJ-MSCs were immunostained with specific antibodies against the surface markers CD31, CD45, CD73, CD90, CD105, and HLA-DR, based on the mesenchymal identity criteria established by the International Society for Cellular Therapy (details in Supplementary Materials) [18]. Cell number and viability were determined by Perfect-Count Microspheres™ (Cytognos, Salamanca, Spain) microbeads and 7-amino-actinomycin D (BD Biosciences, Franklin Lakes, NJ, USA) exclusion method, respectively, following manufacturer's instructions. Acquisition was performed using a FACSCalibur™ flow cytometer (BD, Franklin Lakes, NJ, USA), and data analysed with BD CellQuest™ Pro-software (version 5.2.1.; BD Biosciences, Franklin Lakes, NJ, USA). WJ-MSC potency was evaluated using peripheral blood mononuclear cells (PBMCs) from healthy blood donors (BST), obtained by density gradient (Histopaque-1077; Sigma-Aldrich Inc., St. Louis, MO, USA). To assess cell proliferation, isolated PBMCs were labelled with carboxy-fluorescein diacetate succinimidyl ester (CFSE; Invitrogen, Carlsbad, CA, USA), as previously described [19].

The clinical-grade WJ-MSCs met several safety and quality standards with regards to number of cumulative population doublings, genomic stability, and sterility, which were examined according to the investigational medicinal product dossier approved by the Spanish Agency of Medicines and Medical Devices (AEMPS; PEI16-017). Table 1 summarises the acceptance criteria for all the in-process controls during clinical-grade WJ-MSCs manufacturing.

2.2.2. Vehicle: decellularised, lyophilised and sterilised human pericardium

Human pericardium samples ($n = 35$) were obtained from deceased donors within 24 h post-death, and frozen at −80 °C. Each pericardium was cut into square pieces of 4 × 4 cm (~16 cm^2) and 1 × 1 cm (~1 cm^2).

Decellularisation in the BST-qualified areas was performed as previously reported by our group [14], with some modifications compatible with the quality-by-design approach to ensure human tissue quality (see Supplementary Materials). The procedure was validated using two paired quadrangular pieces of pericardium ($n = 4$ pairs) to demonstrate equivalence between both sizes. Acceptance criteria for each analysed parameter in decellularised pericardia based on the former preclinical construct properties, included DNA content, matrix stiffness, pore size, and microbiological growth (BACT/ALERT® method; BioMérieux, Inc., Durham, NC, USA) (Supplementary Table 1).

Each vehicle batch contained two fragments (~16 cm^2 and ~1 cm^2) of human decellularised, lyophilised, and sterilised pericardium. The ~16 cm^2 was used for PeriCord manufacturing, and the ~1 cm^2 for an in-process quality control (QC; cell viability assessment). Vehicle batch release criteria included negative serological (same as indicated in Table 1 for umbilical cord blood) and microbiological testing of the

Table 1
Acceptance criteria for the manufacturing of clinical-grade WJ-MSCs.

In-process quality control	Acceptance criteria	Manufacturing process
UC blood	Serology: HBsAg, HIV I/II, Lues (TPHA), Chagas, anti-HBc, HCV, anti-HTLV I/II, NAT (HCV-HIV, HBV)	Negative
WJ-MSC expansion step and scale-up to DP	Dose	$\geq 2{\cdot}5 \times 10^7 \pm 20\%$ viable cells/cryotube
	Viability	≥70%
	Karyotype	Non-chromosomal abnormalities
	$CD105^+/CD45^-$ (%)	≥95%
	$CD73^+/CD31^-$ (%)	≥95%
	$CD90^+$ (%)	≥95%
	$HLA\text{-}DR^-$	Informative*
	Mycoplasma	Negative
	Endotoxin	≤1 EU/mL
	Sterility	Sterile
	Adventitious virus	Negative
	Immunomodulation (Potency assay)	>30% Inhibition of PBMC proliferation

Note: DP, drug product; EU, endotoxin units; HBsAg, hepatitis B surface antigen; HBc, hepatitis B core antigen; HBV, hepatitis B virus; HCV, hepatitis C virus; HTLV, human T-cell leukemia-lymphoma virus; HIV, human immunodeficiency virus; NAT, nucleic acid test; PBMC, peripheral blood mononuclear cell; TPHA, *Treponema pallidum* hemagglutination assay; UC, umbilical cord; WJ-MSCs, Wharton's jelly mesenchymal stromal cells.

* HLA-DR for informative purposes only.

pericardial donors, no evidence of microbial growth with the BACTEC™ system (BD, Franklin Lakes, NJ, USA), final regular quadrangular size of 12–16 cm^2, homogeneous density, lack of orifices, residual moisture <10%, and gamma irradiation (25–35 kGy).

2.2.3. PeriCord manufacturing

The development and design of PeriCord (FP) had our preclinical experience as starting point. Different colonisation strategies were assayed in order to replicate the composition of the preclinical construct (2 cm^2) in a larger scale (12–16 cm^2). A final protocol consisting in a sequential cell seeding by sectors onto the vehicle was chosen. Then, PeriCord was an investigational ATMP defined as a human decellularised, lyophilised, and sterilised pericardial matrix (12–16 cm^2) colonised with viable WJ-MSCs in 0.15% v/v PuraStat® (3-D Matrix Inc., Tokyo, Japan) and 10% w/v sucrose (Sigma-Aldrich Inc., St. Louis, MO, USA). PeriCord was manufactured at GMP-certified facilities (BST), following AEMPS-approved procedures (PEI18-140). PeriCord biofabrication involved multiple steps and in-process controls performed on the same day as FP batch release for clinical use (Fig. 2). The main steps were vehicle immobilisation in the primary

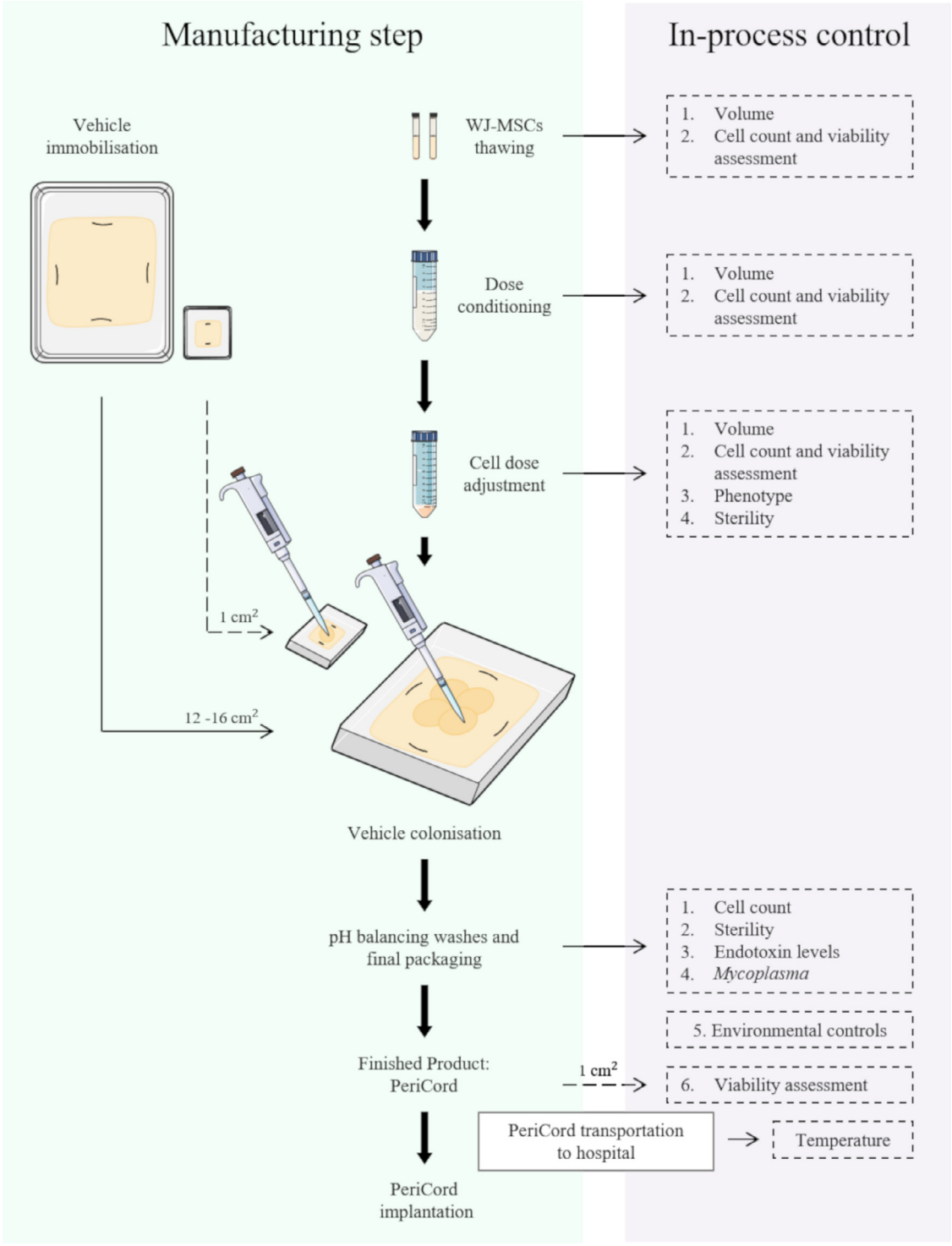

Fig. 2. Schematic of clinical-grade PeriCord manufacturing process, and established in-process QCs.

packaging, WJ-MSCs thawing (2 units of DP), cell conditioning and dose adjustment, vehicle colonisation, and final packaging in a temperature-monitored triple-container system with Plasmalyte®148 solution for PeriCord transportation to the hospital before implantation (details in Supplementary Materials). A small-scale (~1 cm^2) replica of each FP was proportionately manufactured in parallel, for in-process cell viability assessment. We also performed validation of the scale-up procedure, PeriCord manufacturing process, in-process QCs, and FP stability and transportation. In-process QC strategy in the FP include: WJ-MSCs dose calculation, based on cell count method; the microbiological control, endotoxin levels, and *Mycoplasma* test on washing supernatants (as previously described for clinical grade WJ-MSCs batch release); environmental controls (particles and microbiology); and the viability of cells colonising matrix, determined by LIVE/DEAD™ method in the small-scale replica (Fig. 2).The acceptance criteria for initial PeriCord batch certification comprised a dose range of $(7-15) \times 10^6$ total viable WJ-MSCs, ≥70% viability and endotoxin levels ≤4 endotoxin units (EU)/mL.

PeriCord stability was determined by analysing viability of WJ-MSCs colonising matrix with LIVE/DEAD™ method at different time points (from 0 to 96 h), maintaining the FP in the final packaging at RT (n = 3). PeriCord transportation was also validated to evaluate the impact of shipment on the final cell dose. Thus, FP and corresponding small-replica (n = 3 each) were shipped from BST to the Germans Trias i Pujol University Hospital (12-km distance) at RT in a temperature-monitored container, in accordance with P650 Packaging Regulations of the European Agreement Concerning the International Carriage of Dangerous Goods by Road (ADR) for the transport of biological substances, category B (Class UN 3373).

2.3. PeriCord first-in-human surgical implantation

Here we report preliminary data for up to three months following the PeriCord implantation in a roll-in patient from the PERISCOPE trial. The PERISCOPE trial is a first-in-human, phase I, double-blind (patients and clinical cardiologist), single-centre clinical trial (NCT03798353). This study was approved by the AEMPS and the local Ethics Committee from the Germans Trias i Pujol University Hospital (Eudra CT No. 2018-001964-49) and follows the ethical precepts of the Declaration of Helsinki and the Guidelines on Good Clinical Practice specific to ATMPs. The presently reported patient gave signed informed consent prior to enrolment.

The trial will enrol a total of 12 patients with non-revascularisable myocardial scars who are candidates for surgical revascularisation of other myocardial areas, including two roll-in open-labelled patients, and ten randomised patients to a control or treatment group (1:1 ratio, using a computer-generated sequence). Following inclusion in the study (first visit), control patients will undergo coronary artery bypass graft (CABG) for the revascularisable region(s). Treatment patients will undergo the required CABGs and also receive PeriCord applied by surgical glue (Glubran®2, CardioLink, Barcelona, Spain) over the non-revascularisable myocardial scar. Patients will have follow-up visits at one-week post hospital discharge, three, six, and 12 months. The primary endpoint is safety, according to a combination of clinical severe events (death or all-cause rehospitalisation) and severe adverse reaction to the PeriCord. Safety data will be assessed by an independent safety monitoring board. Secondary endpoints include arrhythmias, biomarkers, MRI, and quality of life data.

2.4. Cardiac magnetic resonance imaging data acquisition and analysis

Magnetic resonance imaging (MRI) was performed in a state-of-the-art 1.5T clinical imaging system (InteraDB System; Philips, Eindhoven, NL) with the patient in the supine position, and a 16-element phased-array coil placed over the chest. Images were acquired during breath-holds with ECG gating. We used a segmented k-space steady-state free-precession sequence [repetition time 44·70 ms; echo time 1·26 ms; flip angle 78°; matrix 272; spatial resolution (1·3−1·5) x (1·3−1·5) x 8 mm, depending on the field of view] for cine imaging in parallel short-axis (contiguous slices of 8-mm thickness covering from base to apex), and three long-axis views of the left ventricle. Delayed enhancement images were acquired with a segmented gradient-echo inversion-recovery sequence [repetition time 600−800 ms, depending on the cardiac heart rate; echo time 3·24 ms; flip angle 25°; matrix 256; spatial resolution 1·3 × 1·3 × 8 mm] at matching cine-image slice locations 10 to 20 min after intravenous gadolinium-DTPA administration (0·2 mmol/kg; Gadovist, Bayer Schering Pharma AG, Berlin, Germany) [20]. We optimised the inversion time to null the normal myocardium and adjusted views per segment, and trigger delay according to the patient's heart rate.

All images were reviewed and analysed off-line with a specialised post-processing software (IntelliSpace Portal, Philips, Eindhoven, NL) by an independent operator (A.T.). Left ventricular (LV) endocardial border (papillary muscles were excluded) were manually traced on all short-axis cine images at the end-diastolic and end-systolic frames to determine the LV end-diastolic and LV end-systolic volumes, respectively. LV mass was calculated by subtracting the endocardial volume from the epicardial volume at end diastole and then multiplying by the tissue density (1·05 g/mL) [21,22].

The endocardial and epicardial contours on delayed enhancement images were also outlined manually. Regions of interest (ROIs) were then manually traced in the hyper-enhanced area at place of maximum signal intensity, and in the normal-appearing remote myocardium. As previously described, the areas of hyper-enhancing myocardium were then automatically segmented by using a full-width at half-maximum (FWHM) algorithm [23,24]. Two corrections were required for all automated ROIs. First, microvascular obstruction (defined as hypointensity within a hyperintense region in patients with infarctions) was adjusted to be included as late gadolinium enhancement if present. Second, any obvious blood pool or pericardial partial volume and artefacts were further removed from the ROI.

Scar volume for each slice was calculated as: area scar × slice thickness. The scar mass was expressed as total scar volume × 1·05 g. The scar percentage of myocardium was also expressed as a percentage of the total myocardial volume: volume scar/volume myocardium × 100.

2.5. Statistical analysis

Data are presented as mean ± SEM. Statistical analyses for cytotoxicity experiments were performed using the independent Student's t-test. The paired sample t-test was used to analyse vehicle area reduction and vehicle size comparisons (DNA content, pore size, and roundness in 16 cm^2 vs. 1 cm^2). One-way ANOVA with Tukey's post-hoc correction for multiple comparisons were used for DNA content, pore size, and mechanical data. Non-parametric Friedman and Wilcoxon Signed-Rank tests were used to assess differences in cell viability by sequential colonisation strategy and vehicle size, respectively. Data were analysed using SPSS 21.0.0.0 (SPSS Inc., Chicago, IL, USA), GraphPad Prism 6 (GraphPad Software, San Diego, CA, USA), and SigmaPlot 13 (Systat Software Inc., San Jose, CA, USA). Values were considered significant when $p < 0·05$.

3. Results

3.1. Clinical-grade WJ-MSC production

We obtained clinical grade WJ-MSCs with a 100% success rate (n = 4), yielding a median of $6·4 \times 10^8$ WJ-MSCs, with 30 ± 2 days from initial cord tissue explant culture to DP unit cryopreservation (Fig. 3A). In detail, MCB involved the isolation, selective expansion,

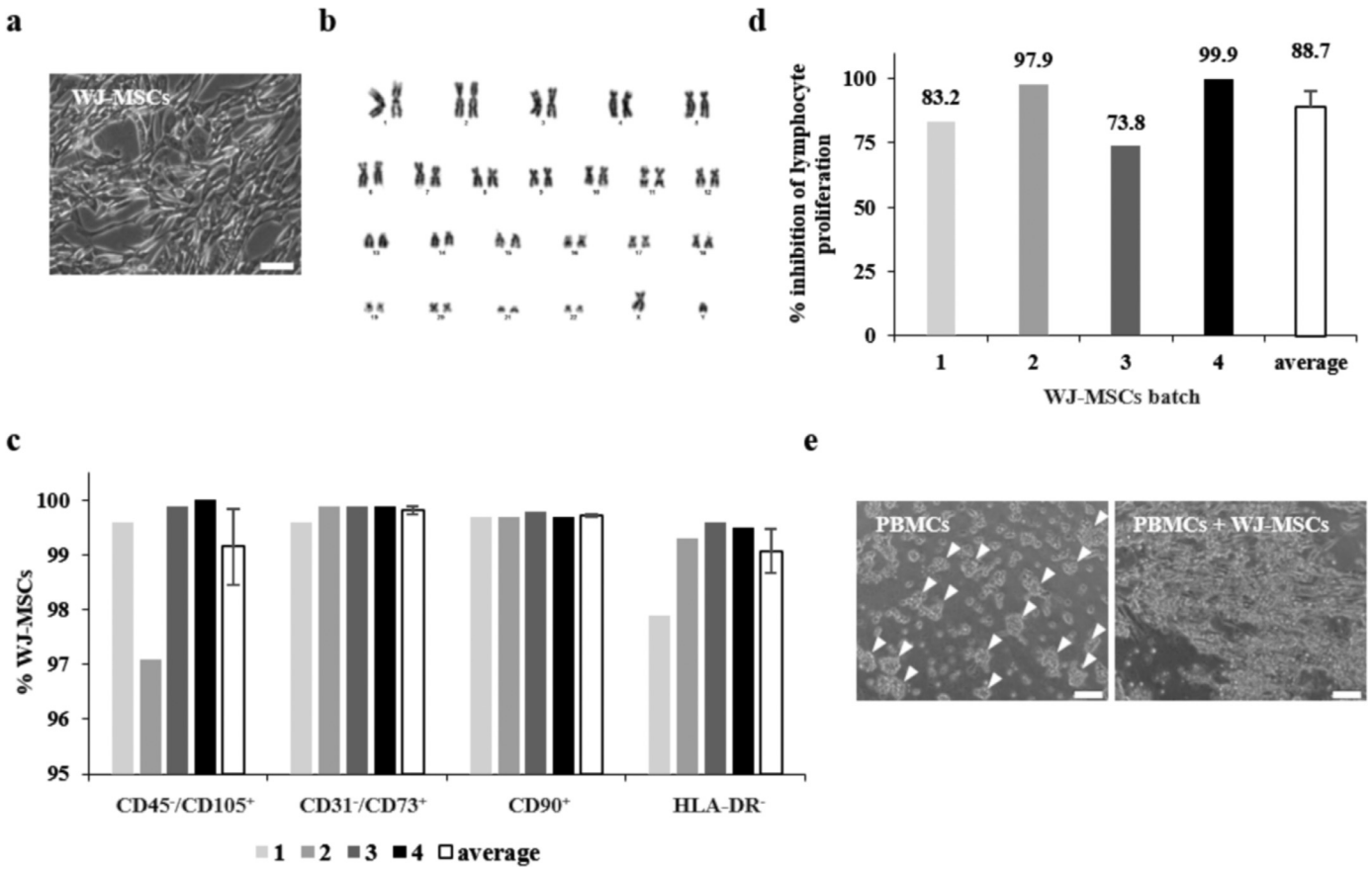

Fig. 3. Clinical-grade WJ-MSC characterisation. (a) Representative microscopic image of expanded WJ-MSCs culture. Scale bar = 100 μm. (b) Normal karyotype of a DP, corresponding to a representative cell line. (c) Immunophenotypic characteristics of four clinical-grade cell batches and average expression (mean ± SEM). (d) Immunomodulation potential measured in four batches of clinical-grade WJ-MSCs, as the capacity to inhibit proliferation of polyclonal stimulated lymphocytes. (e) Microscopic images showing stimulated PBMC clumping, and clump reduction when co-cultured with WJ-MSCs. Arrowheads indicate clumps. Scale bars = 100 μm. PBMCs, peripheral blood mononuclear cells; WJ-MSCs, Wharton's jelly mesenchymal stromal cells.

and cryopreservation of WJ-MSCs. DP encompassed thawing a cryopreserved MCB unit, cell culture expansion, cryopreservation, and QCs. Various in-process controls, including microbiological testing, were performed throughout these steps (Table 1). After expansion, we evaluated sterility using European Pharmacopeia (Eur. Ph.), *Mycoplasma*, and endotoxin tests. In all cell batch productions, a cryopreserved DP unit was generated for use as a control tube for the freeze-thawing process, potency assay, adventitious virus testing, and karyotyping. Observing no evidence of turbidity in any step of the three assayed runs in the Media Fill procedure, we considered the production process aseptic.

Table 2

DP viability was 97·2 ± 0·5% (n = 4), with undetectable levels of endotoxins and *Mycoplasma* DNA. No bacterial contamination or adventitious viruses were detected. To exclude any potential effects of the scale-up process on WJ-MSC genetic stability, we determined G-banding karyotypes at early and late passages. At the cytogenetic level, all karyotypes showed unaltered patterns after accumulating 21 ± 3 cumulative population doublings (Fig. 3B). Phenotypic profiling revealed a MSC-like pattern, with over 95% of cells strongly positive for CD73, CD90, and CD105, and negative for CD31, CD45, and HLA-DR (Fig. 3C). WJ-MSCs' mesenchymal identity was conserved throughout expansion culture, with no differences observed between initial and late passages.

WJ-MSCs of different cell lines or passage numbers did not differ in their ability to inhibit proliferation of polyclonal activated lymphocytes. In all cases, clinical grade WJ-MSCs could inhibit proliferation by 88·7 ± 6·2% (range, 73·8–99·9% inhibition, n = 4; Fig. 3D). At the microscopic level, stimulated PBMCs clusters were reduced only when WJ-MSCs were present, correlating to the immunopotency results obtained (Fig. 3E).

Table 2
Specifications for preclinical construct and finished PeriCord human bioimplant.

	Preclinical construct	PeriCord human bioimplant
	Active ingredient	
Viable cells	Porcine MSCs	Human WJ-MSCs
Density	$0{\cdot}875 \times 10^6/cm^2$	$(0{\cdot}62–0{\cdot}93) \times 10^6/cm^2$
Dose	$1{\cdot}75 \times 10^6$ cells	$(7–15) \times 10^6$ cells
Viability	≥70%	≥70%
	Excipient	
Definition	Vehicle Hydrogel PuraMatrix™ Sucrose Phosphate buffered saline	Vehicle Hydrogel PuraStat™ Sucrose Plasmalyte®®148
Vehicle	Decellularised, lyophilised, and irradiated human pericardium	Decellularised, lyophilised, and irradiated human pericardium
Vehicle size	2 cm^2	12–16 cm^2

Note: MSCs, mesenchymal stromal cells; WJ-MSCs, Wharton's jelly mesenchymal stromal cells.

3.2. Decellularised pericardial matrix processing

The decellularisation protocol generated similar pale pericardial fragments, regardless of the initial sample size (Fig. 4A–C, E, I, and K).

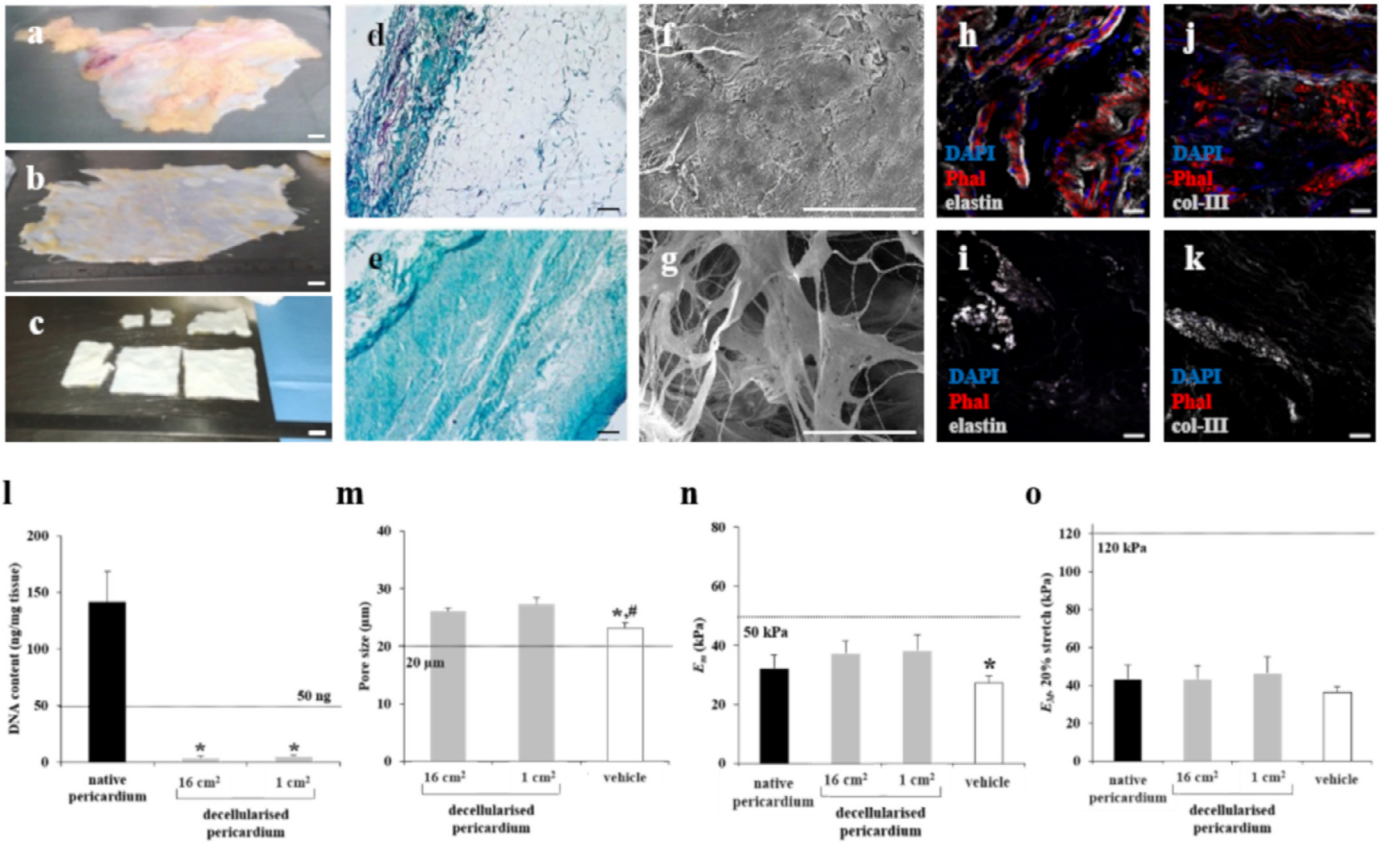

Fig. 4. Pericardial tissue decellularisation. (a) Photograph showing native pericardium from deceased donor. (b) Native pericardium after dissection of superficial adhered adipose tissue. (c) Decellularised pericardial scaffolds after detergent treatment. Scale bars = 1 cm. (d and e) Masson's trichrome staining of native (d) and decellularised (e) pericardium. Scale bars = 100 μm. (f and g) SEM-determined ultrastructure of native pericardium (f) and acellular pericardial matrix (g). Scale bars = 100 μm. (h–k) Representative images of native pericardium (h and j) and decellularised pericardial scaffolds (i and k), showing immunostaining for col-III and elastin (both grey), and cell actin filaments with phalloidin (Phal, red). Nuclei were counterstained with DAPI (blue). Scale bars = 20 μm. (l) Genomic DNA quantification of native tissue, and 16 cm^2 and 1 cm^2 decellularised scaffolds, normalised to scaffold dry weight. *$p < 0{\cdot}05$ [paired Student's t-test], native pericardium vs. decellularised scaffold. (m) Pore size measurements in decellularised pericardial scaffolds and vehicle. (n) Microscopic stiffness (E_m) of pericardium measured with AFM in native tissues and decellularised scaffolds ($n = 4$). (o) Macroscopic stiffness (E_M) of pericardium measured at 20% stretch using tensile testing, for the same tissue conditions. Dashed lines in the graphs indicate the acceptance criteria for each parameter analysed. All data presented as mean ± SEM. *$p = 0{\cdot}046$ [One-way ANOVA and Tukey's post-hoc correction for multiple comparisons], between vehicle vs. decellularised pericardium (1 cm^2). (For interpretation of the references to colour in this figure legend, the reader is referred to the web version of this article.)

Histological analysis with Masson's trichrome staining showed no detectable cells and nuclei (Fig. 4D and E), and immunostaining revealed no cytoskeletal elements or cellular nuclei (Fig. 4H–K). Decellularised scaffolds maintained the intrinsic organisation and spatial three-dimensional distribution of the native matrix fibrils (Fig. 4F and G), and the representative matrix proteins elastin, and type-III collagen were properly stained, indicating preservation of extracellular matrix (ECM) protein components (Fig. 4I and K). Validation of decellularisation was performed by processing four consecutive pericardia, including samples of both ~16 cm^2 and ~1 cm^2. The four decellularised batches met the proposed acceptance criteria for all analysed parameters (Supplementary Table 1). DNA content was <50 ng/mg of decellularised dry tissue, reaching a reduction of nearly 100% in the final decellularised matrix (Fig. 4L). These minimal DNA levels confirmed matrix suitability for clinical use, thus avoiding possible adverse cell and host responses [25]. Matrix dimensions did not significantly differ after decellularisation (2·8 ± 2·9% global area reduction; $n = 5$, $p = 0{\cdot}209$ [paired Student's t-test]). The ~16-cm^2 and ~1-cm^2 decellularised scaffolds exhibited similar pore size (26·0 ± 0·6 μm vs. 27·3 ± 1·2 μm; $p = 0{\cdot}351$ [paired Student's t-test]) (Fig. 4M), and pore roundness ratio (0·5 ± 0·006 vs. 0·5 ± 0·01; $p = 0{\cdot}230$ [paired Student's t-test]). Compared to decellularised scaffolds, the vehicle exhibited smaller pore size (23·1 ± 1·0 μm) and bigger roundness ratio (0·6 ± 0·01), but both parameters met the acceptance criteria demonstrating matrix equivalence.

We evaluated the mechanical properties of pericardial tissue on two scales: micromechanics using atomic force microscopy (AFM) (Fig. 4N), and macromechanics by tensile testing (Fig. 4O). ECM stiffness did not differ after decellularisation compared to native pericardium at the microscale or macroscale. Trehalose incubation, lyophilisation, and sterilisation for obtaining the vehicle induced a slight decrease (~25%) in pericardial scaffold stiffness at the microscale, and a smaller (~15%) non-significant softening at the macroscale ($p = 0{\cdot}384$ [one-way ANOVA]).

Upon validation of the decellularisation protocol, we next validated the manufacture design of the final matrix (vehicle) by processing three consecutive pericardia. The three batches met the proposed acceptance criteria for all analysed parameters in terms of serological and microbiological testing, sterility assessment, final quadrangular size, and residual moisture. Cytotoxicity testing using decellularised, lyophilised, and sterilised pericardial extracts revealed no cytotoxic effects on cell viability (>70%, $n = 3$; $p < 0{\cdot}001$ [Student's t-test]), demonstrating the suitability of the vehicle for clinical use.

3.3. PeriCord cardiac bioimplant: scale-up and manufacturing process

PeriCord with clinically relevant dimensions (12–16 cm^2) comprised human allogeneic WJ-MSCs colonising a human allogeneic decellularised pericardium. Manufacturing process of PeriCord is schematically displayed in Fig. 1. Matrix colonisations were performed from post-thawed sucrose-conditioned cells (2·6 × 10^7 ± 0·1 × 10^7 WJ-MSCs/mL; $n = 37$).

The initial thawed WJ-MSCs' viability (96·1 ± 0·1%) was unchanged following sucrose resuspension (92·4 ± 1·0%), and remained within product specifications even after 16 h at 2–8 °C (88·8 ± 1·6%; n = 20). Cell viability was verified after seeding in both FP (12–16 cm^2) and small-scale replica (1 cm^2), revealing no significant differences in WJ-MSCs' viability when the same post-thawed and sucrose-conditioned cells were seeded into three different matrix batches (FP: 79·6 ± 1·2%; small-scale replica: 78·0 ± 1·1%; p = 0·50 [paired Student's t-test]) (Fig. 5A). Viable cells colonising matrix were also calculated, and no difference between both sizes was observed (Fig. 5B). Moreover, cell viability did not change during sequential cell seeding on different matrix sectors (n = 3 independent matrix batches; p = 0·3 [Friedman test]). Following the defined manufacturing protocol, WJ-MSCs' viability in the FP was 83·1 ± 0·01% (n = 27).

WJ-MSCs' seeding efficiency and dose range in the FP were determined (n = 47) based on the cell retention capacity of pericardial matrices, analysed by calculating the difference between the initial seeded WJ-MSCs and the total recovered cells after pH-balancing washes detailed in the PeriCord manufacturing process. Average WJ-MSCs retention was >90%, corresponding to a density range of (0·62–0·93) × 10^6 total viable WJ-MSCs/cm^2, defining a dose in the range of (7–15) × 10^6 total viable WJ-MSCs/FP.

To validate PeriCord stability in the final packaging, we analysed WJ-MSC viability at different time-points, maintaining the FP at RT (n = 3). PeriCord RT stability period in its final container was defined as the maximum period for maintenance of WJ-MSCs viability at ≥70% (product specification) and was set at 18 h (Fig. 5C).

To evaluate the impact of PeriCord transportation on the cell dose, FP and corresponding small-scale replica (n = 3 each) were manufactured and transported from BST to the Germans Trias i Pujol University Hospital (12-km distance). After transportation, the transport solution (Plasmalyte®®148) was recovered, and the cells counted by flow cytometry. The WJ-MSC dose defined in the batch release was conserved by 98·5% after transport (maximum variation, 4·3%; average dose loss, 1·5%) (Fig. 5D–I).

To validate the manufacture, three consecutive PeriCord batches were processed, all of which met the acceptance criteria for cell dose and viability. Sterility and *Mycoplasma* test were negative or undetectable, and endotoxin levels were <4 EU/mL for all FPs. Environmental microbial controls, pressure levels in qualified areas, and the number of particles fell within the operational range. No other relevant incidences were reported.

3.4. PeriCord cardiac bioimplant: first-in-human patient implantation

PeriCord was implanted in a 63-year-old male patient who suffered an inferior myocardial infarct in 2004, which was conservatively treated. He had a history of tobacco abuse, dyslipidaemia, and mild

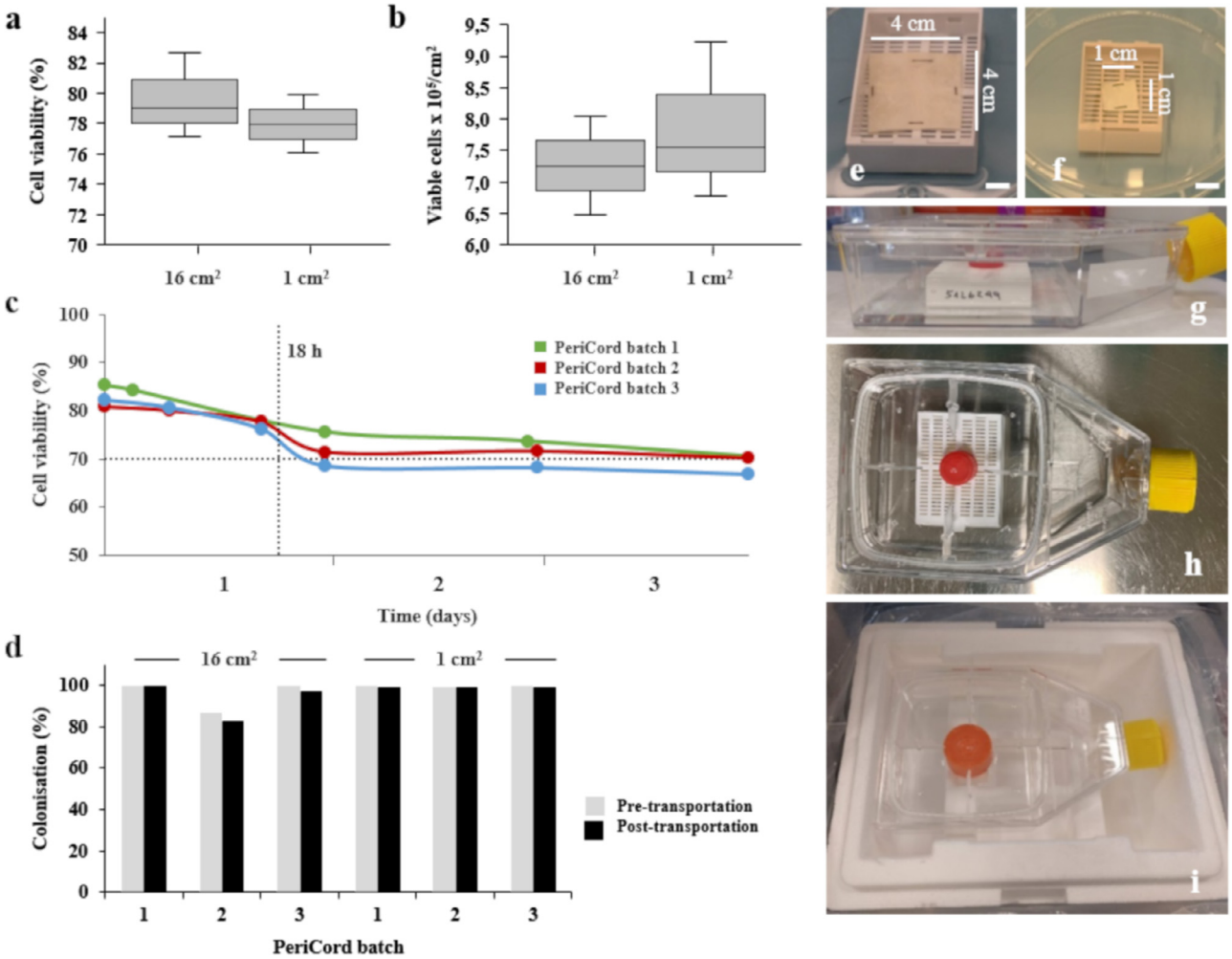

Fig. 5. PeriCord cardiac bioimplant. (a) Cell viability after colonisation was not significantly different between ~16-cm^2 and ~1-cm^2 matrices (n = 3 each). (b) Absolute number of viable colonising cells per cm^2 was also similar in both matrix sizes. (c) Stability testing of PeriCord in final packaging at RT by determining WJ-MSCs' viability using the LIVE/DEAD™ method (n = 3). (d) Transport validation of three PeriCord batches and corresponding small-scale replicas. Colonisation percentage was determined by quantifying cells in recovered pH-balancing washes during manufacturing (pre-transportation), and in the Plasmalyte®148 solution post-transportation. PeriCord (e) and small-replica (f) immobilised in the primary packaging. (g and h) Secondary sterile packaging containing Plasmalyte®148 solution. (i) A third container used for PeriCord transport.

chronic obstructive pulmonary disease with sleep apnoea-hypopnoea syndrome. In March 2019, he presented progressive angina, and coronary angiography showed three-vessel disease, with an occluded right coronary artery, unsuitable for revascularisation. Cardiac MRI showed transmural basal and mid inferior late gadolinium enhancement with subendocardial extension towards the septum and lateral wall (scar mass = 7·8 g, scar size—scar mass normalised by total LV mass- = 5·7%) (Fig. 6E). LV ejection fraction was 40%, with LV end-diastolic volume 177 mL and LV end-systolic volume 106 mL. Having a clear indication for revascularisation of the non-infarcted areas, the patient was offered PeriCord implantation in addition to the planned CABG. After receiving extensive information about the procedure, he gave written informed consent. The first PeriCord manufactured for patient implantation contained $12{\cdot}5 \times 10^6$ viable WJ-MSCs in a 16-cm^2 pericardial scaffold (viability, 85·4%; <0·51 EU/mL) (Fig. 6A). Fig. 6B shows the inferior infarct during open-chest surgery, where the PeriCord was applied and secured with surgical glue at the four edges (Fig. 6C and D, and Supplementary Video 1). The patient underwent CABG to the non-infarcted area at left anterior descending, first diagonal, and oblique marginal. Early post-surgery follow-up was uneventful, except for moderate respiratory distress and surgical suture intolerance unrelated to PeriCord treatment. Post-surgery control echocardiogram showed no signs of pericarditis. No arrhythmic events were registered during the post-operative hospital stay. The patient had a one-week post-discharge visit without significant findings. The PeriCord bioimplant does not carry immunosuppression requirements due to low immunogenicity of the WJ-MSCs [26]. At the three-month follow-up, the patient was alive and without hospital admissions. A three-month cardiac MRI revealed scar mass of 7·1 g (scar size = 5·3%), accounting for ~9% reduction relative to baseline values. In terms of ventricular volumes, LV end-diastolic volume was 159 mL and LV end-systolic volume 96 mL, resulting in reductions of 10% and 9%, respectively, relative to baseline (Fig. 6E and F).

4. Discussion

Here we describe the complex translational process from preclinical testing to first-in-human patient application of the PeriCord engineered 3D cardiac bioimplant, providing proof of principle that PeriCord use in humans is feasible and preliminarily safe (Fig. 1). As we adopt second-generation reparative therapies, such as cardiac tissue engineering, we must be careful to follow regulatory processes to ensure patient safety, and data validity and reproducibility. We will next discuss the characteristics of the two components of the PeriCord as compared with other approaches in the pipeline.

First, we will comment on the cells, i.e., the active ingredient. Irrespective of origin and clinical purpose, cells used for tissue engineering applications in human must comply with the Guidelines on Human Cell-Based Medicinal Products (EMEA/CHMP/410869/2006) from the European Medicines Agency, in terms of the cell population's identity, potency, purity, viability, safety, efficacy, and suitability for the intended use. To date, autologous/allogenic hematopoietic stem cells ($CD34^+$/$CD133^+$), and adult bone marrow/adipose tissue- or WJ-derived MSCs are the only ATMPs listed on the European Medicines Agency website (https://www.ema.europa.eu/en/human-regulatory/marketing-authorisation/advanced-therapies/advanced-therapy-classification/summaries-scientific-recommendations-classification-advanced-therapy-medicinal-products. Accessed July 30, 2019) intended for myocardial regeneration. Of note, none of these are a combined material/cell product. Menasché et al. pioneered the clinical translation of cardiac tissue engineering using

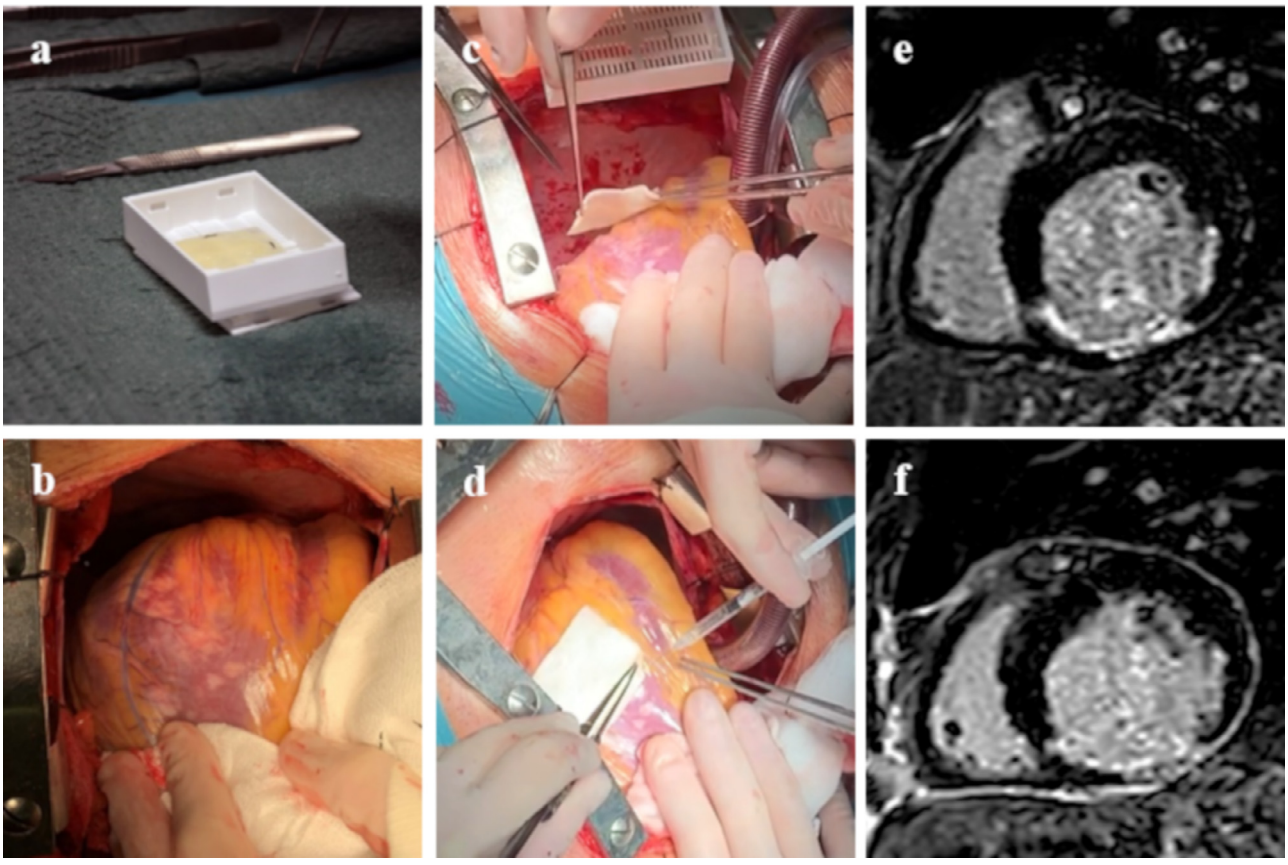

Fig. 6. Surgical PeriCord implantation. (a) PeriCord batch for implantation, in primary packaging at the surgery theatre. (b) Non-revascularisable inferior infarct of the patient. (c and d) Expeditious PeriCord implantation secured by surgical glue droplets at the edges. (e and f) Representative short-axis delayed enhancement cardiac MRI obtained (e) before surgery and (f) at three-month follow-up.

embryonic stem cell (ESC)-derived cardiac progenitors embedded into a fibrin scaffold to treat patients with post-infarct scars [27,28]. However, ethical restrictions and the need for chronic immunosuppression may limit the clinical use of these cells.

Clinical grade WJ-MSCs used in the PeriCord bioimplant could be easily implemented elsewhere. WJ-MSCs exhibit a unique combination of prenatal and postnatal cell properties, and thus constitute an alternative to sources of stem cells with significant barriers of immune rejection, and teratoma formation [29]. This cell type represents an attractive candidate for a readily available off-the-shelf cellular product for several reasons. WJ-MSCs spontaneously secrete numerous pro-angiogenic factors with evidence of functional angiogenic potency in infarcted mammalian hearts [30]. WJ-MSCs are naturally chemoattracted to cardiac tissue, and possess functional ability to populate the ventricular myocardium [31]. In the mini-swine model, WJ-MSCs transplanted by a direct injection into the infarct differentiated into cardiomyocytes and endothelial cells [30]. In addition, WJ-MSCs can be expanded *ex vivo* with high karyotype stability [17], as shown here. Extensive research is being conducted with induced pluripotent stem cell-derived cardiomyocytes within engineered heart tissue grafts. However, to our knowledge, translation to human application has not yet been accomplished [32,33].

Secondly, we will discuss the decellularised pericardium, i.e., the vehicle. In tissue engineering, cells are embedded within a natural or synthetic scaffold, avoiding the harsh infarcted milieu, while improving cell retention and survival compared to direct cell injection [12]. The scaffold biomaterial is crucial, and ideally should closely resemble the physiological cardiac ECM properties. Decellularised cardiac tissues provide a close match to the native, physiological microenvironment with minor changes in stiffness and preserving the composition and three-dimensional framework. Regarding mechanical properties, in a head-to-head comparison of decellularised scaffolds from myocardial and pericardial tissues (prepared following a technique similar to that presently described for the PeriCord), the decellularised pericardial scaffold performed better [16]. showing preserved macromechanical and micromechanical pericardial scaffold properties upon the decellularisation and recellularisation processes. Moreover, the pericardial scaffold demonstrated better cell penetrance and retention, presumably due to bigger pore size [16]. In the context of a preclinical MI swine model, decellularised pericardial engineered grafts of human origin integrated with the underlying myocardium, exhibiting signs of neoinnervation and neovascularisation, and improved cardiac function post-MI [16]. Similar to WJ-MSCs, allogeneic decellularised pericardial matrices could be stored for off-the-shelf clinical use [34].

At present, the manufacturing of a PeriCord cardiac bioimplant by repopulating a pericardial scaffold with WJ-MSCs is labour intensive and requires multiple steps with pre-specified QCs (Fig. 2). It can be achieved within eight working hours, producing a bioimplant valid for clinical use within the following 18 h. The same manufacturing process will be used for each patient enrolled in the phase I PERISCOPE trial, which is currently in the patient enrolment stage.

The reduction in scar mass observed at three months, although remarkable, should be interpreted with caution and should not be used to construe a beneficial functional effect at this point. Indeed, this patient is a roll-in of the PERISCOPE trial, with a primary endpoint set on safety. Cardiac MRI data are part of the secondary endpoints, and include both 3- and 12-month MRI. Nevertheless, cardiac MRI accurately measures scarred and viable myocardium and represents a useful tool for assessing dynamic changes [35]. Relative to the LV volume changes observed, our current understanding suggests they likely result from the concomitant CABG than the PeriCord itself; nevertheless, future implants will shed more light in this issue.

The presently reported PeriCord bioimplant included undifferentiated WJ-MSCs that, at the preclinical level, exhibited abilities to migrate, transdifferentiate, and induce favourable paracrine effects in underlying myocardium [29–31]. Current available data are insufficient to determine whether a cardiac tissue engineered approach requires full *ex vivo* cardiac myocyte and endothelial differentiation, as has been attempted with cardiac-derived embryonic stem cells and induced pluripotent stem cells. This remains an open question for future research.

In conclusion, in this first-in-human preliminary report, we describe the development and testing of a scalable, clinical-size, PeriCord cardiac bioimplant (Fig. 1). The PeriCord bioimplant has several advantages. It constitutes a unique combination of two human allogeneic biological materials that can be stored off-the-shelf and used upon request; does not require host immunosuppression; involves minimal (if any) ethical issues; and incorporates WJ-MSCs, which exhibit karyotype stability, high immunomodulatory activity, lack of tumorigenesis, and substantial proliferative and differentiation potential. Full safety confirmation will be achieved in the ongoing PERISCOPE trial.

Declarations of Competing Interest

There are no conflicts of interest.

Acknowledgements

The authors would like to acknowledge former and current members of both Cell Therapy Service and Barcelona Tissue Bank (Banc de Sang i Teixits, Barcelona) for technical support, advice, and for experimental help in responding to regulatory requests. The authors also thank research nurses for their valuable daily work. We specially thank former and current members of the ICREC Research Lab for their unconditional support. We are very grateful to the donors who donated tissues altruistically, and to the patient who decided to participate in the trial.

Funding sources

This work was supported by the La Marató de TV3 Foundation [201502-30 and 201516-10]; Government of Catalonia: Agency for Management of University and Research Grants (AGAUR) [2017-SGR-483], PERIS Program (Health Department) [SLT002/16/00234 and SLT002/16/00209] and CERCA Program; Catalan Society of Cardiology; “La Caixa” Banking Foundation; grants from the Spanish Ministry of Science, Innovation and Universities (MICINN) [SAF2017-84324-C2-1-R, SAF2017-85574-R and DPI2017-83721-P]; Institute of Health Carlos III (ISCIII) [PI18/00256 and PIC18/00014], Spanish Cell Therapy Network (TerCel) [RD16/0011/0006]; CIBER Cardiovascular [CB16/11/00403] projects, as a part of the National R&D&I Plan, and it was co-funded by ISCIII-Sub-Directorate General for Research Assessment and Promotion and the European Regional Development Fund (ERDF). The funders of the study had no role in study design, data collection, data analysis, data interpretation, or writing of the report.

Author contributions

ABG, CPV, PG, CGM, and SR conceived the initial study. CPV, LRG, and MA designed and performed PeriCord scale-up, analysed, and interpreted experimental data. NNN, and CPV designed and performed decellularisation protocol, and histological experiments under the supervision of EA and AV. EA oversaw the decellularisation protocol logistics. IJ performed mechanical testing experiments and analysed data under the supervision of RF and DN. PG, CGM, MMT, and SR contributed to study design and data analysis. STZ, MIC, LR, and CPV performed PeriCord production and quality controls under the supervision of JV, LRG, and SQ. LRG supervised manufacturing process and PeriCord batch release. PG, CGM, LRG, RC, and CPV prepared documentation for both Regulatory Authority and Local Ethics Committee approvals. PG, and GC assisted in patient recruitment,

clinical study protocol coordination, obtaining consent and sample collection. AT performed cardiac MRI analysis. MLCR, and CMG performed the PeriCord surgical implantation. RF, DN, AV, JGL, SQ, and ABG supervised the work and were responsible for acquisition of funding. CPV, and ABG wrote the first draft of the manuscript that was revised and edited by LRG, MA, PG, CGM, SR, JV, RC, RF, and DN. All authors discussed and revised the final version of the manuscript.

Supplementary materials

Supplementary material associated with this article can be found in the online version at doi:10.1016/j.ebiom.2020.102729.

References

[1] Pfeffer MA, Braunwald E. Ventricular remodeling after myocardial infarction. Experimental observations and clinical implications. Circulation 1990;81:1161–72.
[2] Dib N, Dinsmore J, Lababidi Z, et al. One-year follow-up of feasibility and safety of the first U.S., randomized, controlled study using 3-dimensional guided catheter-based delivery of autologous skeletal myoblasts for ischemic cardiomyopathy (CAuSMIC study). JACC Cardiovasc Interv 2009;2:9–16.
[3] Duckers HJ, Houtgraaf J, Hehrlein C, et al. Final results of a phase IIa, randomised, open-label trial to evaluate the percutaneous intramyocardial transplantation of autologous skeletal myoblasts in congestive heart failure patients: the Seismic trial. EuroIntervention 2011;6:805–12.
[4] Menasché P, Alfieri O, Janssens S, et al. The myoblast autologous grafting in ischemic cardiomyopathy (MAGIC) trial: first randomized placebo-controlled study of myoblast transplantation. Circulation 2008;117:1189–200.
[5] Sanganalmath SK, Bolli R. Cell therapy for heart failure: a comprehensive overview of experimental and clinical studies, current challenges, and future directions. Circ Res 2013;113:810–34.
[6] Gyöngyösi M, Haller PM, Blake DJ, Martin Rendon E. Meta-Analysis of cell therapy studies in heart failure and acute myocardial infarction. Circ Res 2018;123:301–8.
[7] El Omar R, Beroud J, Stoltz JF, Menu P, Velot E, Decot V. Umbilical cord mesenchymal stem cells: the new gold standard for mesenchymal stem cell-based therapies? Tissue Eng B Rev 2014;20:523–44.
[8] Le Blanc K, Mougiakakos D. Multipotent mesenchymal stromal cells and the innate immune system. Nat Rev Immunol 2012;12:383–96.
[9] Roura S, Soler-Botija C, Bagó JR, et al. Postinfarction functional recovery driven by a three-dimensional engineered fibrin patch composed of human umbilical cord blood-derived mesenchymal stem cells. Stem Cells Transl Med 2015;4:956–66.
[10] Monguió-Tortajada M, Roura S, Gálvez-Montón C, Franquesa M, Bayes-Genis A, Borràs FE. Mesenchymal stem cells induce expression of CD73 in human monocytes in vitro and in a swine model of myocardial infarction in vivo. Front Immunolv 2017;8:1577.
[11] Monguió-Tortajada M, Roura S, Gálvez-Montón C, et al. Nanosized UCMSC-derived extracellular vesicles but not conditioned medium exclusively inhibit the inflammatory response of stimulated T cells: implications for nanomedicine. Theranostics 2017;7:270–84.
[12] Hou D, Youssef EA, Brinton TJ, et al. Radiolabeled cell distribution after intramyocardial, intracoronary, and interstitial retrograde coronary venous delivery: implications for current clinical trials. Circulation 2005;112:I150–6.
[13] Teng CJ, Luo J, Chiu RC, Shum-Tim D. Massive mechanical loss of microspheres with direct intramyocardial injection in the beating heart: implications for cellular cardiomyoplasty. J Thorac Cardiovasc Surg 2006;132:628–32.
[14] Prat-Vidal C, Gálvez-Montón C, Puig-Sanvicens V, et al. Online monitoring of myocardial bioprosthesis for cardiac repair. Int J Cardiol 2014;174:654–61.
[15] Gálvez-Montón C, Bragós R, Soler-Botija C, et al. Noninvasive assessment of an engineered bioactive graft in myocardial infarction: impact on cardiac function and scar healing. Stem Cells Transl Med 2017;6:647–55.
[16] Perea-Gil I, Gálvez-Montón C, Prat-Vidal C, et al. Head-to-head comparison of two engineered cardiac grafts for myocardial repair: from scaffold characterization to pre-clinical testing. Sci Rep 2018;8:6708.
[17] Oliver-Vila I, Coca MI, Grau-Vorster M, et al. Evaluation of a cell-banking strategy for the production of clinical grade mesenchymal stromal cells from wharton's jelly. Cytotherapy 2016;18:25–35.
[18] Dominici MK, Le Blanc K, Mueller I, et al. Minimal criteria for defining multipotent mesenchymal stromal cells. The international society for cellular therapy position statement. Cytotherapy 2006;8:315–7.
[19] Grau-Vorster M, Rodríguez L, Del Mazo-Barbara A, et al. Compliance with good manufacturing practice in the assessment of immunomodulation potential of clinical grade multipotent mesenchymal stromal cells derived from Wharton's jelly. Cells 2019;8:E484.
[20] Simonetti OP, Kim RJ, Fieno DS, et al. An improved mr imaging technique for the visualization of myocardial infarction. Radiology 2001;218:215–23.
[21] Kramer CM, Barkhausen J, Flamm SD, Kim RJ, Nagel E. Society for cardiovascular magnetic resonance board of trustees task force on standardized protocols. standardized cardiovascular magnetic resonance imaging (CMR) protocols, society for cardiovascular magnetic resonance: board of trustees task force on standardized protocols. J Cardiovasc Magn Reson 2008;10:35.
[22] Schulz-Menger J, Bluemke DA, Bremerich J, et al. Standardized image interpretation and post processing in cardiovascular magnetic resonance: society for cardiovascular magnetic resonance (SCMR) board of trustees task force on standardized post processing. J Cardiovasc Magn Reson 2013;15:35.
[23] Amado LC, Gerber BL, Gupta BN, et al. Accurate and objective infarct sizing by contrast-enhanced magnetic resonance imaging in a canine myocardial infarction model. J Am Coll Cardiol 2004;44:2383–9.
[24] Flett AS, Hasleton J, Cook C, et al. Evaluation of techniques for the quantification of myocardial scar of differing etiology using cardiac magnetic resonance. JACC Cardiovasc Imaging 2011;4:150–6.
[25] Crapo PM, Gilbert TW, Badylak SF. An overview of tissues and whole organ decellularization processes. Biomaterials 2011;32:3233–43.
[26] Liu S, Yuan M, Hou K. Immune characterization of mesenchymal stem cells in human umbilical cord Wharton's jelly and derived cartilage cells. Cell Immunol 2012;278:35–44.
[27] Menasché P, Vanneaux V, Hagège A, et al. Human embryonic stem cell-derived cardiac progenitors for severe heart failure treatment: first clinical case report. Eur Heart J 2015;36:2011–7.
[28] Menasché P, Vanneaux V, Hagège A, et al. Transplantation of human embryonic stem cell-derived cardiovascular progenitors for severe ischemic left ventricular dysfunction. J Am Coll Cardiol 2018;71:429–38.
[29] Troyer DL, Weiss ML. Wharton's jelly-derived cells are a primitive stromal cell population. Stem Cells 2008;26:591–9.
[30] Zhang W, Liu XC, Yang L, et al. Wharton's jelly-derived mesenchymal stem cells promote myocardial regeneration and cardiac repair after miniswine acute myocardial infarction. Coron Artery Dis 2013;24:549–58.
[31] Lupu M, Khalil M, Andrei E, et al. Integration properties of Wharton's jelly-derived novel mesenchymal stem cells into ventricular slices of murine hearts. Cell Physiol Biochem 2011;28:63–76.
[32] Tiburcy M, Hudson JE, Balfanz P, et al. Defined engineered human myocardium with advanced maturation for applications in heart failure modeling and repair. Circulation 2017;135:1832–47.
[33] Weinberger F, Breckwoldt K, Pecha S, et al. Cardiac repair in guinea pigs with human engineered heart tissue from induced pluripotent stem cells. Sci Transl Med 2016;8 363ra148.
[34] Prat-Vidal C, Bayes-Genis A. Decellularized pericardial extracellular matrix: The preferred porous scaffold for regenerative medicine. Xenotransplantation 2020;27:e12580.
[35] Malliaras K, Smith RR, Kanazawa H. Validation of contrast-enhanced magnetic resonance imaging to monitor regenerative efficacy after cell therapy in a porcine model of convalescent myocardial infarction. Circulation 2013:2764–75.